Petrology, Geochemistry (Isotopic geochemistry)

Using Pb isotopes in surface media to distinguish anthropogenic sources from undercover uranium sources

CrossMark

Kurt Kyser [a,*], Larry Lahusen [b], Garth Drever [c], Colin Dunn [d], Evelyne Leduc [a], Don Chipley [a]

[a] Department of Geological Sciences and Geological Engineering, Queen's University, Kingston ON K7L 3N6, Canada
[b] Uravan Minerals Inc., Suite 204, 2526 Battleford Avenue SW, Calgary AB T3E 7J4, Canada
[c] Houston Lake Mining, 2736 Belisle Drive, Val Caron ON P3N 1B3, Canada
[d] 8756 Pender Park Drive, Sidney BC V8L 3Z5, Canada

ABSTRACT

The response in elemental concentrations and Pb isotopes in various surface media from the Cigar West unconformity-type uranium deposit located at a depth of 450 m were measured to ascertain if element migration from the deposit can be detected at the surface. The media included clay-size fractions separated from the A2, B and C soil horizons, and tree cores and twigs from black spruce (*Picea mariana*) and jack pine (*Pinus banksiana*) trees. Lead isotopes were used to trace any effect on the surface media from the deposit at depth because the $^{207}Pb/^{206}Pb$ ratios in the ore are < 0.1, whereas the background values in the basin are > 0.7 and modern anthropogenic Pb from aerosols are near 0.9. The tree cores record their lowest and therefore most radiogenic $^{207}Pb/^{206}Pb$ ratios of < 0.7 near the surface projection of the deposit and associated structures, particularly in tree rings that predate any exploration and drilling activity in the area. The median $^{207}Pb/^{206}Pb$ ratios increase in the order C, B soil horizon clays, tree cores, A2 soil clays and twigs because of the increasing contribution of common Pb with high ratios from anthropogenic sources that affect the shallowest media the most. Although this anthropogenic Pb as well as that from the background dominates the composition of all media at the surface and the contribution from the deposit at depth is diminished toward the surface, ore-related Pb is still present as a few percent of the composition of pathfinder elements and Pb isotopes.

© 2015 Académie des sciences. Published by Elsevier Masson SAS. All rights reserved.

1. Introduction

A basic tenet in exploration geochemistry is that elevated concentrations of metals and compounds in ore deposits will disperse with time and be recorded as aberrations in normal background levels. The basis of this theory is well founded in the principles of chemistry because the tendency of all systems is to become random and equal in energy so that high concentrations will disperse with time over vast areas, even if kinetics slow this process. Exploration geochemistry proves that this concept is valid because there are numerous cases where "leakage" of elements from deposits at depth is evident (Cameron et al., 2004, 2010; Kelley et al., 2004). The new challenges are identifying those particular elements and media that truly reflect dispersion from ore deposits below the surface (Coker, 2010). Given the paucity of recent discoveries of ore deposits at the surface (Marlatt and

Kyser, 2011), most new discoveries will be made at depth, and thus we must be able to "see" them from the surface with geochemistry (Cohen et al., 2010).

A variety of different surficial media are used in exploration for undercover mineral deposits with a variety of different selective leaches to target specific phases or elements (Cornelius et al., 2007; Hall et al., 1996). One such medium is vegetation, including trees and their various organs collected as part of biogeochemical exploration. Biogeochemistry was first adapted as a tool for mineral exploration in response to new technologies needed for mineral exploration methods that were cheaper and more time efficient (Dunn, 2007a; Warren et al., 1952). Plants can reveal the geochemistry of the substrate through amalgamation of lateral substrate geochemical signatures from stream sediments and aquifers through their root systems, and directly through penetration of the roots into the underlying substrate (Dunn, 2007b). The particular mechanism or mechanisms a plant employs mostly depends on the kind of root system it has, such as spreading lateral roots or deep sinker roots. A variation on the use of plants is the use of trees cores, which reflect a time sequence of element migration in the area (Kozuskanich et al., 2009; Watmough, 1997). A temporal record is required due to the global influence of anthropogenic activity (Kelley and Hudson, 2007; Lahd Geagea et al., 2008). Tree rings that reflect pre-global industrialization because of their age should be a more reliable record of elements that may have migrated from deposits below as opposed to those that were deposited from atmospheric sources (Kozuskanich et al., 2009).

The utility of Pb isotopes to distinguish geogenic and anthropogenic Pb and metal sources has been demonstrated in a study of rock, soil, and plant samples collected at 3 km intervals along a 120 km long transect across the city of Oslo, Norway. These media record a general increase towards the north, the prevailing wind direction, in $^{207}Pb/^{206}Pb$ ratios, and an increase in Pb concentrations around urban areas. In addition, low variability in plant samples and O-horizon soil profiles compared to rocks and mineral soils, were observed along the transect and interpreted as mass fractionation of Pb as a result of biological processes, therefore resulting in less radiogenic and more constant Pb isotopic compositions that differ from the underlying mineral soils (Reimann et al., 2008). However, other studies on media such as peat bogs on local, regional or global scales demonstrate that anthropogenic Pb emitted in the atmosphere from leaded gasoline, coal burning and metallurgy has been dispersed worldwide, and this Pb has a high $^{207}Pb/^{206}Pb$ near 0.9. Preanthropogenic Pb isotopic compositions in continental archives of atmospheric deposition like peat bogs and soils (Kylander et al., 2009; Shotyk and Krachler, 2010; Shotyk et al., 1998) indicate that the Pb isotopic signature is regionally, not locally, defined. Thus, the Pb isotopic signatures of the biogenic samples from Oslo more likely reflect 20th century anthropogenic Pb and local geogenic background Pb than mass-dependent or mass-independent fractionations, which are exceedingly small for heavy elements. The relationship between Pb concentrations and isotopic compositions in these media indicates mixing between two end-members, one of which is geogenic Pb, and the other having $^{207}Pb/^{206}Pb$ near 0.9 that are anthropogenic.

In this study, we examine secondary dispersion of radiogenic Pb isotopes and elements that are mobilized from the deeply buried unconformity-related uranium deposit at Cigar West in the Athabasca Basin in Canada, and how this Pb is manifest in media at the surface. We also compare the Pb isotopic compositions and concentration of elements in black spruce (*Picea mariana*) and jack pine (*Pinus banksiana*), a study similar to one that Jean Carrignan did with snow. The proposed mechanism by which elements migrate to the surface involves transport by gaseous complexes and compounds released by microbial activity in the ore to eventually adhere to clay minerals within surficial soils and tills (Plant et al., 1988). Thus, the unique radiogenic Pb isotopic compositions and pathfinder elements from the ore will be recorded in surficial clay and vegetation (Kelley et al., 2006; Leslie et al., 2014). Numerous multimedia, multi-element, multi-digestion geochemical surveys over known uranium showings and deposits in and around the Athabasca Basin in northern Saskatchewan suggest that secondary dispersion processes result in anomalies in pathfinder elements in certain soil components and vegetation over the deposit and along deposit related fractures (Bonham-Carter and Hall, 2010; Dunn, 1984; Earle and Drever, 1983; Earle and Sopuck, 1989). To trace the radiogenic Pb and pathfinder element signal originating from the high-grade uranium deposit over 450 m to the surface, sampling involved collecting tree cores, as well as twigs and needles and A2, B and C soil horizons from which clay fractions were separated, over and far from the deposit. Trees represent an advatageous sampling media for exploration geochemistry because they occur in most places in Canada and their root systems are vast, thereby collecting mobile elements over a significant width and depth. In addition, their chemical compositions should reflect a chronology of their chemical environment.

2. Geological considerations

The Cigar Lake and Cigar Lake West deposits are located in the eastern part of the Athabasca Basin and hosted in the Athabasca Group, which unconformably overlies the transition between the western Wollaston and eastern Mudjatik basement domains (Fig. 1A). The basal Wollaston domain includes graphitic units, with many deposits located at the metamorphosed contact between Archean granitoid gneisses and these graphitic metapelite units. The basal sequence of the Athabasca Group (Manitou Falls and Fair Point formations) consists of permeable coarse- to medium-grained, hematite-rich conglomerate and sandstone with paleocurrent directions predominantly from the east (Hoffman, 1988; Ramaekers et al., 2007). The basal portion of the Manitou Falls Formation is composed of coarse-grained conglomerate beds with attributes that reflect deposition in high energy braided streams, or alluvial fan settings. The lower coarse-grained interval is overlain by finer grained sandstone with minor conglomerate that is marked by abundant trough cross bedding and
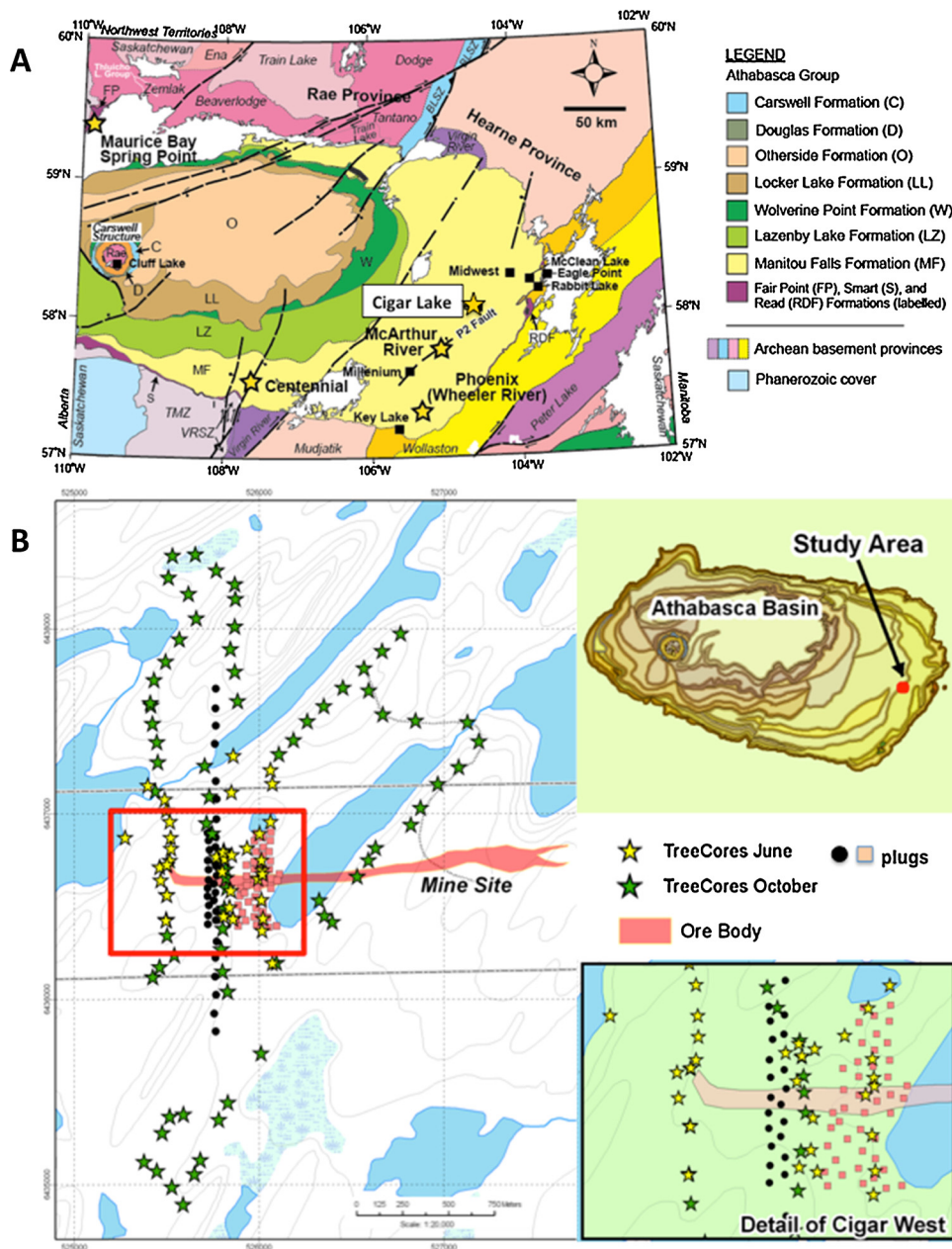
Fig. 1. (Color online.) A. General geology of the Athabasca Basin in N. Saskatchewan, Canada, and location of the Cigar Lake deposit (modified from Hoffman, 1988; Ramaekers et al., 2007). B. Location of the Cigar Lake West area in the Athabasca Basin. Stars indicate locations of tree cores and other symbols are tree plugs not discussed in this study.

relatively rare siltstone layers. This middle interval represents deposition in more distal braided stream environments, and due to the much better sorting, has coarse-grained textures, more extensive quartz cement, and lower hydraulic conductivity. The sandstone layers that make up the upper third to half of the Manitou Falls Formation consist of medium-grained sandstone with abundant ripple marks, rare thin mudstone layers and mud rip-up clasts. This sandstone is consistent with deposition in lower energy distal braided stream systems to possibly braid deltas. The detrital material that makes up the Manitou Falls sandstone units is composed of 95–100% well rounded quartz with minor muscovite and rare heavy minerals, such as Fe-Ti oxides. The absence of feldspar and rarity of any other minerals further suggests intense weathering in the source area and relatively long distance transport.

The Manitou Falls Formation is unconformably overlain by a succession of less permeable marine sandstone, phosphatic siltstone, and phosphatic mudstone layers, the

Lazenby Lake Formation, Wolverine Point Formation, respectively, which are in turn overlain first by sandstone (Locker Lake, Otherside and Tuma Lake Formations, and the William River Subgroup), then by shale (Douglas Formation), and finally by stromatolitic dolomite (Carswell Formation). These marine units in conjunction with the unconformities would be ideal environments in which evaporated seawater could permeate into the lower units.

The deposits at Cigar Lake are complex-type deposits hosted by clay-altered Athabasca Group sandstone and conglomerate within 50 m of the unconformity (Bruneton, 1993). A minimum age for the mineralization is 1467 ± 63 Ma (Fayek et al., 1997). The clay-size fraction of the alteration halo associated with the Cigar Lake uranium deposit consists of illite with subordinate kaolinite, sudoite (Al-chlorite), Fe-chlorite, hematite, and traces of an illite-chlorite mixed-layer mineral (Percival et al., 1993). Complex deposits are characterized by Ni, Co, Cu, Pb, Zn, and Mo sulfides and arsenide minerals in addition to uraninite, grading up to 80% U in high-grade areas (Cuney and Kyser, 2009). Clay-bounded, massive ore occurs as elongate pods and linear ore bodies of a high-grade core and lower grade halo along the unconformity and just above it in the overlying Athabasca Group. At the Cigar Lake deposit, one pod is 1.9 km long, 50 to 100 m wide and 20 m thick (Bruneton, 1987).

Portions of the Cigar Lake deposit, and specifically Cigar West, offer excellent sites for this study, with the presence of high-grade uranium mineralization known at depth, a database of historical geochemical surveys at the proximal Cigar Lake deposit, and relatively undisrupted surface conditions providing access to soil horizons and vegetation. There is also a relatively consistent nature of the geomorphology, vegetation and drainage across the study area. Cigar West is a relatively undisturbed length of 50 m wide mineralization that extends 500 m to the west of Cigar Lake (Fig. 1B). The mineralization, which is accompanied by high concentrations of Ni, As, Mo, and Co, straddles the unconformity, extending vertically into the sandstone along structures. The sandstone thickness is about 450 m with an alteration halo extending upward less than 200 meters from the mineralization. Glacial till is approximately 10–15 m thick and consists of boulders and fine sand with minor amounts of silt. The soil substrate in the boggy area is dominantly sand derived from erosion of the till.

The area over the Cigar West zone of mineralization is typical of Canadian Shield Boreal forest. Jack pine is the dominant tree species, with scattered black spruce, birch, and tamarack in wet areas. Mountain alder, dwarf birch, Labrador tea, minor leather leaf and reindeer moss dominate the underbrush and ground cover. The 50 by 50 m grid area was predominantly flat with gradual elevation gains to the north and south sections of the Cigar West grid. Within the 100 by 100 m grid and background 200 by 200 m grid sections, topography changes were more pronounced (Fig. 1B).

Historical drill core from six holes was available for sampling and a structural interpretation based on drilling and geophysical compilations was available from Assessment files. These structures may act as conduits for migration of elements from the ore deposit to the surface environment above.

3. Sample collection and analytical techniques

Soils and vegetation were sampled from 340 stations and tree cores from 220 sites (Fig. 1B). At most of the 340 stations, the A and B soils were available for collection, but only 283 sites were suitable for C-horizon soils. Sample collection was at 50 m spacing on an offset grid for 250 m on either side of the projected vertical extension of the Cigar West zone of mineralization, located beneath more than 450 m of Athabasca sandstones. To the north and south of this zone, the grid was expanded by 3 km to an offset grid of 100 m between sample stations.

At each site, a stainless steel shovel was used to expose the A, B and C soil horizons. Approximately 1 kg of the A-, B-horizon and C-horizon were collected with a stainless steel scoop, placed in individual zip-lock bags and labelled. These soil horizons were selected because they are easily accessible from the surface and easy to identify. The clay-sized fractions ($< 2 \mu$m) were extracted from the soil samples at the Queen's Facility for Isotope Research (QFIR) and analyzed by aqua regia digestion followed by analysis for 53 elements and Pb isotopes using Q-ICP-MS at Acme Labs. The technique for Pb isotope measurement at Acme Labs is similar to that at QFIR, except for the type of ICP-MS used, with three times longer counting times for mass 204 relative to all other masses. Clay minerals were separated because they have reactive, charged surfaces and significant surface area compared to other phases in soils (Velde, 1992). Data quality proved to be excellent, with RSD better than 10% for most elements.

In addition, vegetation samples at each site were collected from the ends of the bottom branches of the nearest black spruce and a few jack pine trees using stainless steel snips and placed in a sentry sample bag, filling the bag to capacity (~ 200 g). The strategy behind analysis of vegetation samples is that this is a demonstrated medium for recording anomalies from uranium deposits at depth observed in previous studies (Dunn, 1984). All black spruce and jack pine vegetation samples were oven-dried at 80 °C for 24 h. Black spruce twigs and selected jack pine twigs and needles were sent to Acme Labs for reduction to ash at 470 °C to burn off all of the organic components. A 0.25-g portion of ash was digested in aqua regia and the solution analyzed by Q-ICP-MS by Acme Labs.

Tree cores were collected from both black spruce (*Picea mariana*) and jack pine (*Pinus banksiana*) trees using a Suunto Tree Corer (Fig. 1B). The largest trees were cored through the widest part of the tree trunk at chest height. All cored trunk wood was retrieved, wrapped in paper, sealed with tape and labelled. In June 2009, 110 cores were collected over the deposit and in September 2009, 110 cores of mainly spruce were collected to better define the background. During the June sampling program, two core samples were collected from each tree in an east–west and a north–south orientation, but only a north–south-oriented tree core sample was collected in September because results indicated a difference of less than 20% for all elements between the two orientations of cores from the same tree (Table 1).

The diameters of the trees ranged over 8–18 cm, averaging 12 cm. The cores were lightly sanded to reveal

Table 1

Average differences in % and standard deviations (%) of element concentrations and Pb isotope ratios measured between east–west- and north–south-oriented cores from the same tree. Also shown is the number of samples that have concentrations of these elements above detection limits.

	Pine (EW–NS)			Spruce (EW–NS)		
	Aver diff %	St dev (%)	n	Aver diff %	St dev (%)	n
Al	3.7	8.7	11	0.0	9.8	38
Au	9.5	18.1	2	11.0	7.5	3
B	0.1	15.7	13	1.6	11.0	52
Ba	1.9	6.7	13	0.4	5.0	52
Ca	1.0	4.2	11	0.9	4.4	48
Cd	1.0	10.6	10	1.3	9.9	29
Ce	−2.1	10.3	7	16.0	24.6	14
Co	1.0	9.7	2	1.0	12.7	27
Cr	−4.3	13.9	9	0.4	14.4	48
Cs	0.5	8.6	5	0.6	4.1	30
Cu	4.6	13.7	11	0.4	9.8	47
Fe	−3.5	16.0	11	0.5	14.3	48
K	−3.2	16.5	11	0.7	4.3	46
La	7.4	22.8	6	1.3	12.4	6
Li				0.4	11.2	20
Mg	0.4	5.7	11	0.8	8.6	49
Mn	0.0	6.3	11	0.2	4.7	42
Mo				1.5	9.6	14
Na	−2.5	14.3	12	0.4	14.9	51
Ni	2.2	14.9	11	0.8	12.9	48
P	−0.1	9.0	11	0.4	8.2	48
Pb	1.3	15.1	11	1.0	12.7	44
Rb	0.8	5.6	11	0.1	5.3	48
S	−3.8	15.8	11	0.1	4.0	45
Sb	16.5	27.3	3	1.6	16.2	15
Se	2.9	11.1	4	1.6	8.2	9
Si	22.0	39.6	2	0.7	7.9	21
Sr	1.2	5.5	11	0.4	4.5	47
Ti	5.2	17.4	9	3.6	14.2	39
U				2.7	16.0	44
V	2.6	8.9	3	3.1	10.8	19
W	5.3	17.6	12	4.2	11.9	19
Zn	1.3	5.8	11	0.3	4.7	48
$^{207}Pb/^{206}Pb$	0.6	3.8	13	0.1	2.9	52
$^{206}Pb/^{204}Pb$	−1.4	5.0	13	0.4	4.5	52
$^{207}Pb/^{204}Pb$	−0.8	2.3	13	0.5	3.5	52
$^{208}Pb/^{204}Pb$	−0.6	2.1	13	0.5	3.7	52

Aver diff %: average differences in %; St dev (%): standard deviations (%); EW: east–west; NS: north–south.

the rings and remove surface contamination. The ages of the trees ranged from 18–150, with average of 39 years. The widths of each ring was measured to verify that that they decreased toward younger rings, thus indicating that the tree had not been unduly stressed, which can affect metal uptake (Shortle et al., 1997; Watmough, 1997, 1999). Analysis of tree core material from trees that predate the drilling and surface activities at Cigar West (1980–1983) was preferred, although about 35% of the trees were younger than 1983. Rings from 5–20-year intervals of growth dating prior to 1990 were then removed for analysis.

Samples of the years selected were first cleaned with deionized water in glass vials in an ultrasonic bath for 10 minutes. All samples were placed in a 60 °C oven to dry overnight. Approximately 100–200 mg of sample was weighed into Savillex™ screw top beakers and 2 mL of concentrated distilled nitric acid added. The containers were placed on a 70 °C hotplate for 3 h for total digestion, then five drops of hydrogen peroxide were added to remove dissolved organics and produce a clear solution after heating to 70 °C on a hotplate overnight. Several samples required more than treatment with peroxide to remove all dissolved organic material. The samples were then dried at 70 °C, redissolved in 2% HNO$_3$ and diluted to 1–5 g with 2% HNO$_3$ with 1 ppb Indium as an internal standard to correct for fluctuations in sample flow-rate, matrix effects and instrument sensitivity. Metal concentrations and Pb isotopic compositions were determined at QFIR with a Thermo Finnigan Element 2 high-resolution magnetic sector inductively coupled plasma mass spectrometer (ICP-MS), which is capable of both low-level analyses as well as high-quality Pb isotopic compositions. The Pb isotope ratios were calculated using the signal intensities (counts/s) in low-resolution mode, with corrections for interferences from Hg and mass fractionation monitored using Tl in the solutions and externally with in-house and NIST Pb isotope standards (NBS 981, normal Pb and NBS 983, radiogenic Pb). For each sample, 204, 206, 207, 208 and 202 were measured, blank subtracted and ^{204}Pb was corrected for ^{204}Hg interference using ^{202}Hg. Mass bias corrections were not necessary as NIST standard values were near to certified values and well within the limits necessary in order to distinguish samples in the study. Concentrations were corrected for instrument drift and matrix using ^{115}In as an internal standard and external calibration for element concentrations and blank subtraction. In total, 219 core intervals were analyzed at QFIR for all elements, with Al, B, Ba, Ca, Cr, Cu, Fe, K, Mg, Mn, Na, Ni, P, Pb, Rb, S, Sr, W, U, Zn, and Pb isotopes detected in most samples (Tables 2 and 3).

Table 2

Median concentrations and reproducibility for analytical duplicates of black spruce.

Element	Median concentrations (ppb or ng/g)	Aver diff %	n
Al	2750	9.9	6
B	42,000	6.2	6
Ba	19,000	5.3	6
Ca	350,000	5.3	6
Cr	200	21.5	6
Cs	20	5.0	3
Cu	700	13.2	6
Fe	2300	18.2	6
K	300,000	5.0	6
Mg	90,000	4.9	6
Mn	100,000	4.7	6
Na	100,000	9.4	6
Ni	100	18.8	6
P	35,000	12.2	6
Pb	40	8.9	6
Rb	1000	4.6	6
S	42,000	7.5	6
Si	25,000	9.8	6
Sr	3000	7.0	6
W	100	22.9	6
Zn	8000	6.5	6
$^{207}Pb/^{206}Pb$	0.87	1.8	5
$^{206}Pb/^{204}Pb$	25.31	7.0	5
$^{207}Pb/^{204}Pb$	20.52	5.9	5
$^{208}Pb/^{204}Pb$	52.47	6.1	5

Aver diff %: average differences in %.

Table 3

Average, minimum, maximum, median and standard deviation of element concentrations and Pb isotopic compositions in pine and spruce tree cores.

Element	Pine						Spruce					
	AVERAGE	MIN	MAX	Median	St dev	Count	AVERAGE	MIN	MAX	Median	St dev	Count
Al	1966	691	3738	1675	971	24	2157	269	6109	2224	1022	95
As	14	6	24	13	9	3	19	4	33	22	14	5
Au	19	4	66	11	22	7	20	9	41	19	9	15
B	10,147	1409	30,538	5600	8880	25	23,369	1567	88,907	21,733	17,006	103
Ba	5902	1149	19,607	3024	4961	26	13,806	1997	27,846	14,343	6684	106
Bi	DL	DL	DL	DL	DL	0	11	3	65	6	17	12
Ca	135,602	73,849	289,765	102,747	62,181	24	380,709	76,837	879,181	395,925	167,775	103
Cd	43	9	123	36	30	23	25	5	181	13	38	46
Ce	11	4	43	6	11	16	7	5	11	8	2	9
Co	9	7	14	8	2	7	14	5	43	11	8	56
Cr	74	21	202	70	48	24	222	21	1672	156	245	103
Cs	10	5	20	9	5	10	19	4	44	19	11	62
Cu	461	177	1387	376	278	24	730	113	1752	728	383	102
Fe	12,543	1856	37,993	10,524	10,495	24	36,504	2551	154,123	25,843	34,617	104
Gd	8	4	9	8	2	4	9	5	12	8	3	9
Hg	DL	DL	DL	DL	DL	0	21	12	31	21	7	13
K	145,109	59,107	289,747	99,531	76,755	23	214,079	55,047	392,716	236,413	79,708	101
La	11	4	39	7	10	11	14	3	50	7	18	6
Li	27	21	34	27	9	2	52	21	124	48	21	37
Mg	69,556	25,409	150,766	44,938	42,118	24	100,285	20,273	252,815	98,510	46,888	105
Mn	11,054	2558	36,101	7167	9660	23	54,714	9249	161,640	50,662	33,651	90
Mo	DL	DL	DL	DL	DL	DL	32	7	233	21	41	42
Na	43,249	5490	144,240	25,248	39,552	26	66,019	5811	739,064	44,167	96,217	106
Nb	33	20	48	32	14	3	89	25	207	80	51	18
Nd	6	4	7	7	2	3	5	4	7	6	1	3
Ni	115	23	272	71	84	24	223	19	1131	179	199	105
P	13,211	1390	34,845	10,725	8458	24	11,475	595	53,326	7573	9942	104
Pb	26	4	139	20	29	24	40	5	256	34	34	86
Rb	535	202	1045	374	277	24	922	281	2703	916	439	105
S	17,717	7149	38,267	11,782	10,590	23	29,018	5175	79,405	30,066	14,761	102
Sb	6	4	8	6	2	4	23	4	276	8	55	39
Se	9	4	21	8	5	11	1455	27	2572	1818	901	12
Si	1336	1096	1535	1357	184	4	12,620	1318	60,590	2742	15,228	68
Sr	2351	800	7537	1382	1761	24	3672	530	7513	3836	1796	104
Ti	33	5	131	22	30	21	65	7	587	45	76	82
Tl	6	4	8	5	1	6	7	4	13	6	2	33
U	24	3	92	19	22	25	23	5	112	17	17	73
V	DL	DL	DL	DL	DL	0	18	7	57	14	12	43
W	DL	DL	DL	DL	DL	0	132	17	472	100	101	61
Zn	2955	768	10,081	2063	2299	23	6806	1236	19,140	6543	3498	105
Zr	24	12	38	22	13	4	58	20	280	28	90	8
U	24	3	92	19	22	25	23	5	112	17	17	73
$^{207}Pb/^{206}Pb$	0.66	0.43	0.80	0.71	0.11	26	0.77	0.44	0.89	0.79	0.09	106
$^{206}Pb/^{204}Pb$	28.90	20.22	43.41	25.54	6.83	26	26.57	20.02	49.49	24.77	6.57	104
$^{207}Pb/^{204}Pb$	18.50	16.11	25.79	18.29	2.06	26	19.77	16.19	34.14	18.15	4.08	104
$^{208}Pb/^{204}Pb$	43.58	38.80	63.03	42.02	5.03	26	48.51	39.42	83.55	43.83	10.66	104

Min: minimum; Max: maximum; St dev: standard deviation; DL: below detection limit.

The quality of the analyses was monitored using a tree core standard prepared by QFIR (Kozuskanich et al., 2009) and NIST 1547 peach leave standard, each of which were measured for every 15 samples. The practical detection limit for all elements, including Pb isotopes, is 0.01 ppb. The Pb isotopic compositions recorded by the tree ring standard indicate accuracies in the $^{207}Pb/^{206}Pb$ ratio of ± 0.03 (2σ), $^{206}Pb/^{204}Pb$ of ± 1.77 (2σ), $^{207}Pb/^{204}Pb$ of ± 1.22 (2σ), and $^{208}Pb/^{204}Pb$ of ± 3.22 (2σ) for complete analysis of the tree rings and even better for the clay separates. The Pb isotopic compositions were also monitored using solutions prepared from the dissolution of a Pb wire from international CRMs for Pb isotopes, NIST-981, a common Pb standard and NIST-983, a radiogenic Pb standard. These standards were analyzed for every 6 samples and their results reflect how

precisely and accurately the HR-ICP-MS can analyze a 1 ppb solution. The precision of the $^{207}Pb/^{206}Pb$ ratios based on these CRMs is 0.4% and the accuracy is ± 0.01, whereas those for the $^{206}Pb/^{204}Pb$, $^{207}Pb/^{204}Pb$, and $^{208}Pb/^{204}Pb$ are 2.5% and ± 0.22.

4. Results

There are marked differences in the average concentration of some elements in pine relative to spruce samples (Table 3). Tree rings from pine have less than half the concentrations of B, Ba, Ca, Cu, Fe, Hg, K, Mg, Mn, Mo, Na, Ni, Rb, Se, Si, Sr and Zn than do spruce tree cores. Other elements have similar concentrations in both types of trees (Table 3). The Ag and Cs concentrations are higher in the

spruce than pine twigs, whereas Al, Cd, Cr, Sb, Se and Tl are higher in pine than spruce twigs. Different organs of vegetation are known to sequester different concentrations of some elements (Dunn, 2007a; Watmough, 1997), so that recognition of anomalies from a deposit at depth must be organ specific. However, the fractionation of Pb isotopes is minimal given the small differences in their masses, so Pb isotopic compositions in both species of tree are comparable.

Two different core directions (east–west and north–south) were collected for each tree in June 2009, to evaluate the homogeneity of particular elements in the tree cores and to evaluate the reproducibility of the analyses. With the exception of a few elements, all elements and Pb isotopic compositions in both pine and spruce are homogeneous throughout rings of the same year (Table 1). Moreover, the standard deviations for all elements are comparable to analytical uncertainties of less than 20% deduced from analyses of the standard wood and samples from opposite sides of the same core. Exceptions are Ce and Sb in spruce and La, Sb and Si in pine, in large part due to their low concentrations.

The isotopic composition of Pb can be a definitive indicator of migration of components from a variety of ore deposits (Bell and Franklin, 1993; Dickson et al., 1987; Gulson, 1983; Holk et al., 2003; Leybourne et al., 2009), especially for U deposits because the decay of U in high concentrations results in only ^{206}Pb and ^{207}Pb. As this radiogenic Pb moves during secondary migration into the environment away from the deposit, it mixes with common background Pb, thereby producing Pb isotopic compositions that have elevated $^{206}Pb/^{204}Pb$ and $^{207}Pb/^{204}Pb$ ratios, but lower $^{207}Pb/^{206}Pb$ ratios (Holk et al., 2003). Although the levels of Pb are low in the samples of the tree cores, averaging only 40 ppb (40 ng/g) in spruce (Table 3), and the precision is a few percent, the range in Pb isotopic compositions in the tree cores is significant (Fig. 2). For example, the $^{207}Pb/^{206}Pb$ ratios, which are the most accurate and precise ratios of all the Pb isotopes to measure by a mass spectrometer because of the similarity in their masses, range from 0.4 to 0.9 in the tree cores (Fig. 2). The population of $^{207}Pb/^{206}Pb$ ratios is not normally distributed, and cumulative probabilities define at least four potential populations, with the lowest, most radiogenic population having $^{207}Pb/^{206}Pb$ ratios less than 0.6 (Fig. 2). Samples with $^{207}Pb/^{206}Pb$ ratios less than 0.7 are normally considered radiogenic in the Athabasca Basin (Holk et al., 2003), so several of the tree cores record radiogenic Pb.

The $^{207}Pb/^{206}Pb$ ratios of the selected media are all quite variable, although those closest to the surface, namely the spruce twigs (vegetation) and clays from the A2 soils are less radiogenic than the other media, with most samples having $^{207}Pb/^{206}Pb$ ratios of common Pb near 0.9 (Fig. 3). In effect, the median $^{207}Pb/^{206}Pb$ ratios are lowest and hence more radiogenic in the clays from the B and C soils, and the tree cores have a number of radiogenic samples, although the median $^{207}Pb/^{206}Pb$ ratio is less radiogenic than the clays from the B and C soils (Fig. 3). Element concentrations are much lower in tree cores and vegetation samples, including Pb and U contents, whereas clays from A2 and C
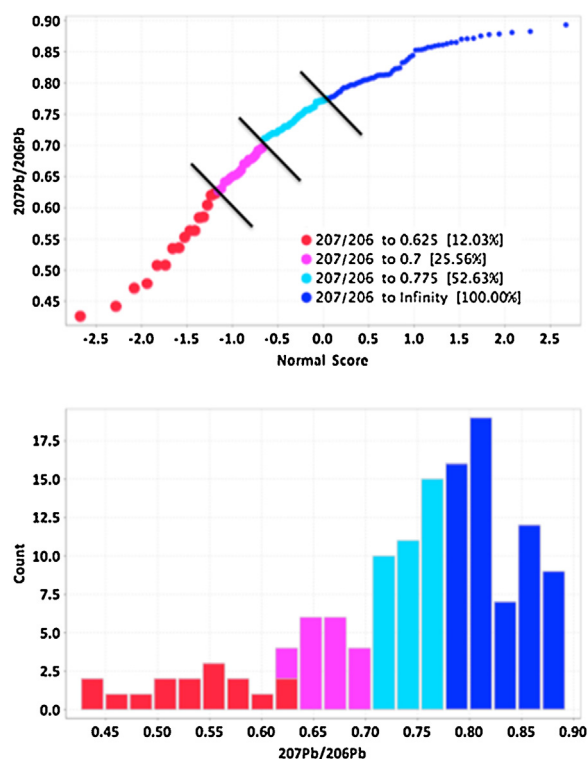

Fig. 2. (Color online.) Cumulative probability plot of $^{207}Pb/^{206}Pb$ ratios in spruce tree cores (top) and histogram of $^{207}Pb/^{206}Pb$ ratios, both showing distinct populations of ratios, with those in red and purple having significant radiogenic Pb isotopic compositions of < 0.7.

soils tend to have the highest Pb and U concentrations of the surface media (Fig. 3). Although $^{207}Pb/^{206}Pb$ ratios tend to lower and thus more radiogenic values with decreasing Pb concentrations in tree cores, the clay samples from all soils record lower and thus more radiogenic $^{207}Pb/^{206}Pb$ ratios with increasing U concentrations (Fig. 3).

Many elements display regular relationships with $^{207}Pb/^{206}Pb$ ratios in spruce tree cores. Exponential correlations with $^{207}Pb/^{206}Pb$ ratios include B, Ba, Ca, Cs, K, Mg, Mn, S, Tl, Zn and inverse relationship with $^{206}Pb/^{204}Pb$ and $^{207}Pb/^{204}Pb$ ratios (Fig. 4) and REEs. Since the lowest $^{207}Pb/^{206}Pb$ ratios are the most radiogenic (Holk et al., 2003) and are most likely to be derived from the ore body, these elements actually correlate inversely with radiogenic Pb. Thus, there are negative exponential correlations between radiogenic Pb derived from the deposit in the tree cores and the alkaline earths, alkali metals, B, and some chalcophile elements, so that negative anomalies of these elements are spatially related to the deposit. It is noteworthy that the $^{207}Pb/^{206}Pb$ ratios do not correlate with U concentrations in the tree rings because these elements should have different mobility characteristics.

The spatial distribution of $^{207}Pb/^{206}Pb$ ratios in the tree rings indicates that most of the lowest ratios are near the projection of the deposit to the surface (Fig. 5) and that background samples have the highest, least radiogenic ratios. Because trees sample such a large area of the surface with their root systems, they are an integrating medium.
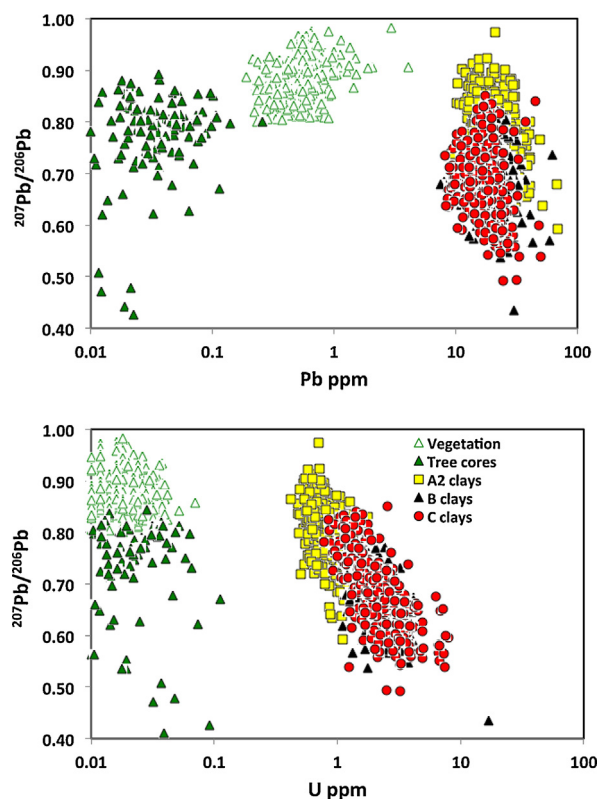
Fig. 3. (Color online.) Relationship between $^{207}Pb/^{206}Pb$ ratios and log Pb and U concentrations in clays from A2, B, C soils and spruce tree twigs (Vegetation) and tree cores. Tree cores and clays from B and C soils have the lowest and most radiogenic $^{207}Pb/^{204}Pb$ ratios < 0.7, whereas clays from A2 soils and vegetation have higher and more common Pb ratios. Tree cores and vegetation samples have the lowest Pb and U contents, similarly for most other elements, whereas clays from A2 and C soils tend to have the highest Pb and U concentrations of the surface media.

The tree cores show a similar spatial distribution in their $^{207}Pb/^{206}Pb$ ratios to the clays from the B and C soils, but not with the A soils or the vegetation samples.

5. Discussion

Differences in the concentrations of many elements between black spruce and jack pine in this study are similar to other studies that compare metal concentrations between species (Anderson et al., 2000; Cheng et al., 2007; Watmough, 1999) that indicate each species generally responds differently to the concentrations of metals in the environment. Many species are not useful as temporal records of their environment because of translation of elements among the rings (Cheng et al., 2007; Lageard et al., 2008; Watmough and Hutchinson, 2003), including Pb isotopes in some species (Patrick and Farmer, 2006). Although there are differences in the concentrations of some metals between both species, the relative spatial distribution of many elements in both is similar when there is overlap, particularly Pb isotopes. Thus, Pb isotopes, which do not record any isotopic fractionation in natural systems (Kyser, 2012; Shotyk and Le Roux, 2005; Weiss

et al., 1999), should be similarly recorded in the tree rings of the two species.

Translocation of elements in black spruce is not evident in this study given that the element concentrations and Pb isotopic compositions are similar in both north–south- and east–west-oriented cores (Table 3). Other studies exploring for VMS deposits also found no evidence for translocation of elements in black spruce (Kozuskanich et al., 2009), although sampling of sapwood in spruce can result in significant differences in parts of the same ring especially if the tree was stressed (Prohaska et al., 1998). The ring widths measured in this study were the same for the samples taken from different oriented cores, thus indicating a lack of stress for the age of the rings sampled, and sapwood was avoided in most samples.

The spatial distribution of $^{207}Pb/^{206}Pb$ ratios in the tree core samples indicate that the most radiogenic values are in trees near the projection of the deposit to surface or structures that transect the deposit at depth (Fig. 6). The $^{207}Pb/^{206}Pb$ ratios in clay fractions from the A2, B and C soils are similarly distributed, and especially demarcate the NE-trending structures (Fig. 7).

The tree rings sampled were from ages prior to significant anthropogenic activity in the Cigar Lake area. The $^{207}Pb/^{206}Pb$ ratios correlate with many elements including B, Ba, Ca, Cs, K, Mg, Mn, S, Sr, Tl, Zn and Pb, and because of the "biofilter" effect, these elements, or the lack thereof, define the deposit as negative anomalies relative to background. Similarly, elemental concentrations in spruce twigs delineated U, Bi, REE, Ba, Th, Co, Ni, Bi, Sn, Li, Mo, V, Fe and Al that best reflect the presence of U mineralization concealed beneath 450 m of Athabasca sandstone. However, the vegetation samples have a larger component of common Pb, which has high $^{207}Pb/^{206}Pb$ ratios.

The exponential correlation between radiogenic Pb and the elements recorded in the tree cores is not as pronounced in other media in this study, although the spatial response of the Pb isotopes in each medium is similar (Fig. 6). Tree cores are the only media that record negative anomalies in elements over the deposit, including the twigs of spruce trees. This reflects biofiltering associated with incorporation and distribution of elements into tree wood and other tissues. The low concentrations of many elements in trees over the deposit relative to the background may reflect the types of microbes affecting the flux of gases from the deposit as well as the ability of the organism to uptake specific elements (Watmough, 1997). Regardless of the process to produce negative anomalies in some element concentrations in the tree cores, when combined with radiogenic $^{207}Pb/^{206}Pb$ ratios that are definitive indicators of a U-rich source, they clearly demarcate the position of the deposit at depth (Fig. 5), and just as importantly, indicate areas that are less prospective. Those $^{207}Pb/^{206}Pb$ ratios that are not directly associated with the projected deposit at the surface are associated with faults that cut the deposit (Figs. 5 and 6), which are likely conduits for element migration from the deposits to the surface. Those elements in tree cores that correlate exponentially with $^{207}Pb/^{206}Pb$ ratios also correlate well with each other. Other notable correlations
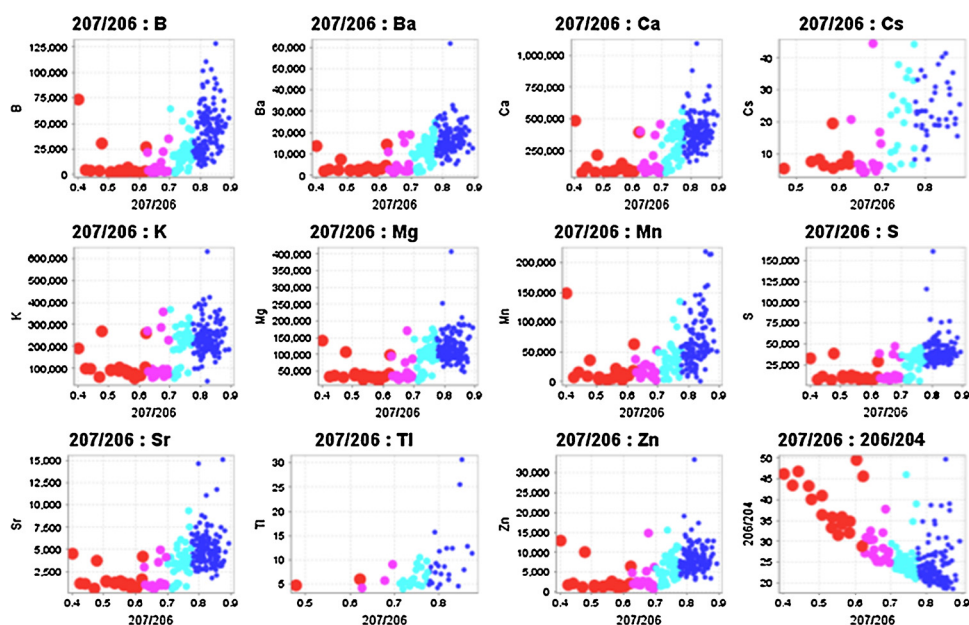
Fig. 4. (Color online.) Relationship between elemental concentrations of B, Ba, Ca, Cs, K, Mg, Mn, S, Sr, Tl, Zn concentrations and ^{206}Pb/^{204}Pb ratios in spruce tree rings. Colors and sizes denote populations of ^{207}Pb/^{206}Pb ratios as defined on Fig. 2, with largest circles representing the lowest, most radiogenic ^{207}Pb/^{204}Pb ratios. Curved relationships indicate mixing between two major reservoirs, one with high ^{207}Pb/^{206}Pb ratios and high element concentrations and low ^{206}Pb/^{204}Pb ratios and the other with lower, more radiogenic ^{207}Pb/^{206}Pb ratios indicative of a Pb from a U-rich source.

include those among the transition metals (Co, Fe, Ni), which are all used as coenzymes in plant systems and are normally incorporated in the tree in direct proportion to their concentration in the environment. The exponential relationships between element concentrations and ^{207}Pb/^{206}Pb ratios are indicative of mixing between two distinct sources, one with high ^{207}Pb/^{206}Pb ratios and low elemental concentrations and the other with higher, common Pb isotopic compositions and higher elemental concentrations.

Ideally, the ^{207}Pb/^{206}Pb ratios of all the surface media should have similar ranges and be similarly distributed spatially. However, there is a relationship between distance from the surface of the sample and the ^{207}Pb/^{206}Pb ratio wherein the clay fraction from the B and C soils have the lowest, and therefore more radiogenic

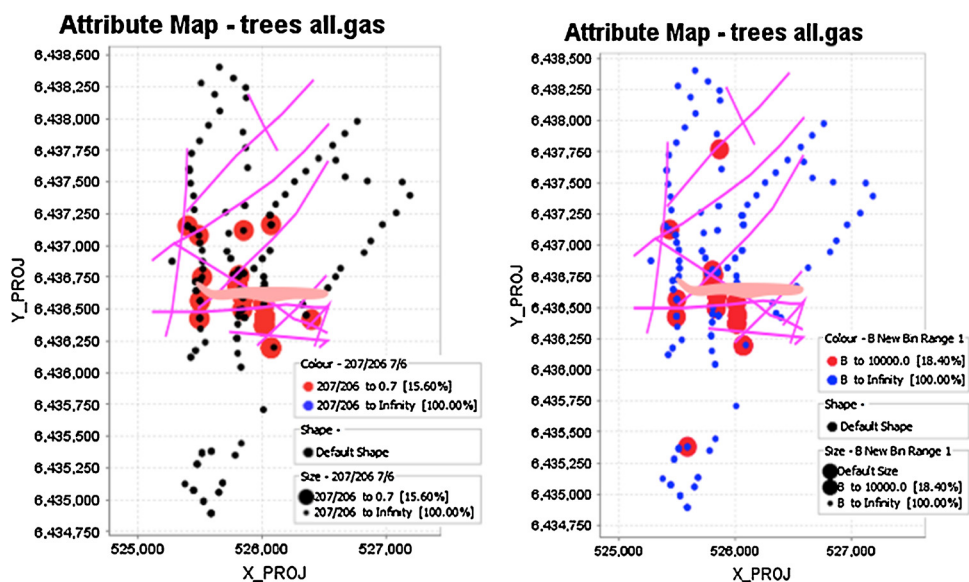**Fig. 5.** (Color online.) Spatial distribution of ^{207}Pb/^{204}Pb ratios (left) and inverse B concentrations in spruce tree cores. The large circles on the left diagram reflect ^{207}Pb/^{204}Pb ratios < 0.7, whereas those on the right diagram are B contents < 10,000 ppb, less than 10% of the population. Projection of the deposit to the surface is also shown, as are faults as lines.
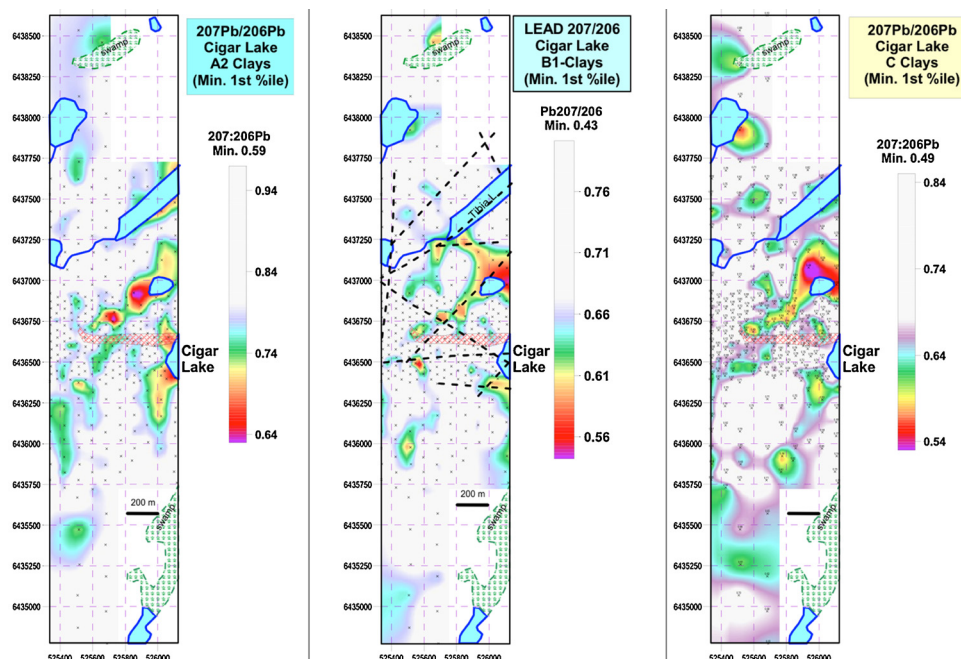
Fig. 6. (Color online.) Spatial distribution of ^{207}Pb/^{206}Pb ratios in A2, B1 and C clays from soils at Cigar West. Other elements with very similar distributions include Ni, Co, REEs, Sr, Tl, K, Rb, Cs.

ratios (Fig. 7), although many away from the projection of the deposit have common Pb isotopic ratios (Figs. 5 and 6). In reality, the media closest to the surface, namely the vegetation and A2 soil clays, have on average more common ^{207}Pb/^{206}Pb ratios (Fig. 7). The tree cores have among the most variable ^{207}Pb/^{206}Pb ratios.

These media actually sample their environment on different spatial and temporal scales. The B and C soil samples reflect spot samples of the till at depth, and should reflect components of the till and elements migrating to the surface laterally and from below. The A2 soil is also a spot sample, but of the more recent environment

Fig. 7. (Color online.) Histogram of ^{207}Pb/^{206}Pb ratios for surface media in the Cigar West area. The media include clay fractions separated from the C, B, A2 soil horizons, as well as tree cores and vegetation from black spruce trees. Median values are lowest, and thus have more radiogenic Pb from a U-rich source, in the C and B soils, less radiogenic in the A2 and tree core samples, and are least radiogenic in the vegetation samples, the latter being closest to the surface.

dominated by deposition of components from above. The trees sample a large area at depth, sampling components coming from below and in the till, but also from the recent environment near the surface, hence the large range in ^{207}Pb/^{206}Pb ratios. The vegetation samples reflect an environment dominated by recent aerosols deposited on their surfaces and by components deposited on the near surface in the past few years. Thus, the sample media that reflect the most recent Pb in the environment are vegetation and A2 soils, which are closest to the surface. These media are most susceptible to Pb deposited from aerosols, i.e. "from above". Those with more radiogenic Pb isotopic compositions such as the B and C soils, reflect Pb from deeper sources, including those from radiogenic Pb and pathfinder elements migrating from the deposit at depth, especially along fractures. The common Pb recorded in the vegetation and less so in the A2 soils is consistent with anthropogenic common Pb deposited from smelting of Pb ores and gasoline.

The isotopes of Pb have a demonstrated utility in tracing the impact of anthropogenic Pb having high ^{207}Pb/^{206}Pb ratios on the environment. For example, the terrestrial record of common Pb having high ^{207}Pb/^{206}Pb ratios near 0.9 is recorded in soils, lake sediments and snow from Canada (Gallon et al., 2003; Simonetti et al., 2000a; Simonetti et al., 2000b; Tessier et al., 2005). A chronology of the concentrations and isotopic compositions of oceanic Pb in the North Atlantic Ocean for the past 220 years (Boyle et al., 2009) in annual bands of corals that grew in coastal seawaters near Bermuda and from seawater samples collected from the North Atlantic since 1980 indicate that anthropogenic Pb emissions in this area reflect the industrialization of North America since 1840 and the introduction of leaded gasoline in 1920 until
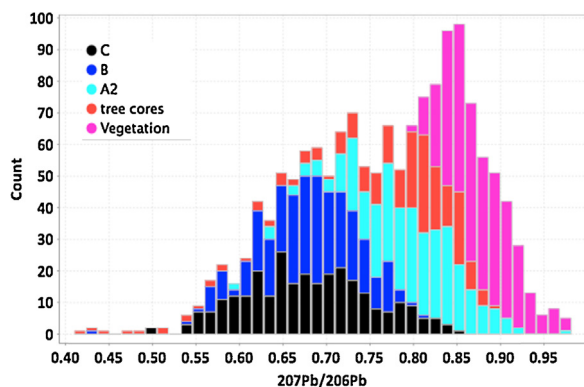
its cessation by the late 1990s. Lead isotope ratios are the least radiogenic before 1900 due to the early dominance of Upper Mississippi Valley Pb ore in the USA. After 1900, $^{207}Pb/^{206}Pb$ ratios increase slightly until 1970 when sources of common Pb were phased out in the United States.

The tree cores record their lowest and therefore most radiogenic $^{207}Pb/^{206}Pb$ ratios of < 0.7 near the surface projection of the deposit and associated structures, particularly in tree rings that predate any exploration and drilling activity in the area. The median $^{207}Pb/^{206}Pb$ ratios increase in the order C, B soil horizon clays, tree cores, A2 soil clays and twigs because of the increasing contribution of common Pb with high ratios near 0.9 from anthropogenic sources that affect the shallowest media the most. Although this anthropogenic Pb as well as that from the background dominate the composition of all media at the surface and the contribution from the deposit at depth is diminished toward the surface, ore-related Pb is still present as a few percent of the composition of pathfinder elements and Pb isotopes.

The results from Cigar Lake West are similar to others involving multimedia such as rock, soil, and plant samples collected through the city of Oslo, Norway, that showed differences among the media, with the highest $^{207}Pb/^{206}Pb$ ratios recorded in the media closest to the surface. Multiple media record the affects from anthropogenic Pb emitted in the atmosphere from leaded gasoline, coal burning and metallurgy and dispersed worldwide (Bindler et al., 1999, 2004; Kylander et al., 2009). The relationship between Pb concentrations and isotopic compositions of the surface media at Cigar Lake West indicates mixing between two end-members, one of which has the lowest $^{207}Pb/^{206}Pb$ and reflects Pb that has migrated from the uranium deposit at depth, and the other having high $^{207}Pb/^{206}Pb$ ratios that are anthropogenic. Thus, exploration geochemistry requires an understanding of environmental geochemistry, and vice versa.

6. Conclusions

Radiogenic (low) $^{207}Pb/^{206}Pb$ ratios define the deep Cigar West deposit at the surface in tree rings from black spruce (*Picea mariana*) and jack pine (*Pinus banksiana*), as well as in other media. Radiogenic (low) $^{207}Pb/^{206}Pb$ ratios correlate inversely with many elements including B, Ba, Ca, Cs, K, Mg, Mn, S, Sr, Tl, Zn and Pb, that define the deposit as negative anomalies relative to background. Thus, Pb isotope ratios and depletions in many other elements in tree rings are definitive indicators of U mineralization at depth in tree rings.

The Pb in surface media at Cigar West is sourced from three major reservoirs: the deposit at depth, the Athabasca Group sandstones and till, and common Pb deposited at the surface, most likely from anthropogenic activity. This is reflected in the mean $^{207}Pb/^{206}Pb$ ratios of each medium wherein medium at the surface such as A2 soils, or a medium that has recently accumulated atmospheric Pb at the surface such as vegetation, have common Pb ratios. In contrast, those media more removed from the surface and thus recent atmospheric Pb accumulations, but are more

influenced by geogenic Pb, including radiogenic Pb from the deposit at depth, have more variable and lower $^{207}Pb/^{206}Pb$ ratios. Thus, exploration geochemistry requires knowledge of the environmental geochemistry, even in areas as remote as the Athabasca Basin in Canada.

References

Anderson, S., Chappelka, A.H., Flynn, K.M., Odom, J.W., 2000. Lead accumulation in *Quercus nigra* and *Q. velutina* near smelting facilities in Alabama, USA. Water Air Soil Pollut. 118, 1–11.

Bell, K., Franklin, J.M., 1993. Application of lead isotopes to mineral exploration in glaciated terrains. Geology (Boulder) 21, 1143–1146.

Bindler, R., Brannvall, M.L., Renberg, I., Emteryd, O., Grip, H., 1999. Natural lead concentrations in pristine boreal forest soils and past pollution trends: a reference for critical load models. Environ. Sci. Technol. 33, 3362–3367.

Bindler, R., Renberg, I., Klaminder, J., Emteryd, O., 2004. Tree rings as Pb pollution archives? A comparison of Pb-206/Pb-207 isotope ratios in pine and other environmental media. Sci. Total Environ. 319, 173–183.

Bonham-Carter, G., Hall, G., 2010. Multimedia Techniques for Direct Detection of Covered Unconformity Uranium Deposits in the Athabasca Basin. Canadian Mining Industry Research Organization (CAMIRO) Journal Project 08E01. Toronto, 280 p.

Boyle, E.A., Kelly, A.E., Reuer, M.K., Goodkin, N.F., 2009. Lead concentrations and isotopes in corals and water near Bermuda, 1780–2000. Earth Planet. Sci. Lett. 283, 93–100.

Bruneton, P., 1987. Geology of the Cigar Lake uranium deposit (Saskatchewan, Canada). Spec. Publ.- Sask. Geol. Soc. 8, 99–119.

Bruneton, P., 1993. Geological environment of the Cigar Lake uranium deposit. Can. J. Earth Sci. 30, 653–673.

Cameron, E.M., Hamilton, S.M., Leybourne, M.I., Hall, G.E.M., McClenaghan, M.B., 2004. Finding deeply buried deposits using geochemistry. Geochem. -Explor. Environ. Anal. 4, 7–32.

Cameron, E.M., Leybourne, M.I., Reich, M., Palacios, C., 2010. Geochemical anomalies in northern Chile as a surface expression of the extended supergene metallogenesis of buried copper deposits. Geochem. -Explor. Environ. Anal. 10, 157–169.

Cheng, Z., Buckley, B.M., Katz, B., Wright, W., Bailey, R., Smith, K.T., Li, J., Curtis, A., Geen, A.V., 2007. Arsenic in tree rings at a highly contaminated site. Sci. Total Environ. 376, 324–334.

Cohen, D.R., Kelley, D.L., Anand, R., Coker, W.B., 2010. Major advances in exploration geochemistry, 1998–2007. Geochem. Explor. Environ. Anal. 10, 3–16.

Coker, W.B., 2010. Future research directions in exploration geochemistry. Geochem. -Explor. Environ. Anal. 10, 75–80.

Cornelius, M., Porto, C.G., Dunn, C.E., Butt, C.R.M., Oates, C., Coelho, R., 2007. Soil and biogeochemical signatures of the Aripuana base metal deposit, Mato Grosso? Brazil. Geochem. -Explor. Environ. Anal. 7, 179–192.

Cuney, M., Kyser, K., 2009. Recent and not-so-recent Developments in Uranium Deposits and Implications for Exploration, Short Course Series Vol. 39. Mineralogical Association of Canada, Québec, 258 p.

Dickson, B.L., Gulson, B.L., Snelling, A.A., 1987. Further assessment of stable lead isotope measurements for uranium exploration, Pine Creek Geosyncline, Northern Territory, Australia. J. Geochem. Explor. 27, 63–75.

Dunn, C.E., 1984. Geochemical studies in the Athabasca test area, Saskatchewan. CIM Bull. (1974) 77, 72.

Dunn, C.E., 2007a. Biogeochemistry in Mineral Exploration. Elsevier, Amsterdam, The Netherlands.

Dunn, C.E., 2007b. New perspectives on biogeochemical exploration. Proc. Decenn. Int. Conf. Miner. Explor. 5, 249–261.

Earle, S., Sopuck, V., 1989. Regional lithogeochemistry of the eastern part of the Athabasca Basin uranium province, Saskatchewan. In: Muller-Kahle, E. (Ed.), Uranium Resources and Geology of North America. International Atomic Energy Agency, Technical Document TECDOC-500, Vienna, pp. 263–269.

Earle, S.A.M., Drever, G.L., 1983. Hydrogeochemical exploration for uranium within the Athabasca Basin, northern Saskatchewan. J. Geochem. Explor. 19, 57–73.

Fayek, M., Janeczek, J., Ewing, R.C., 1997. Mineral chemistry and oxygen isotopic analyses of uraninite, pitchblende and uranium alteration minerals from the Cigar Lake Deposit, Saskatchewan, Canada. Appl. Geochem. 12, 549–565.

Gallon, C., Gobeil, C., Tessier, A., Carignan, R., 2003. Stable Pb isotopes and PAHs as indicators of lead contamination sources in a lake of the Rouyn-Noranda area. In: XIIth International Conference on Heavy Metals in the Environment, May 26, 2003–May 30, 2003, I ed. EDP Sciences, Grenoble, France, pp. 505–508.

Gulson, B.L., 1983. Evaluation of lead isotopes in soils in exploration for concealed base metal mineralization. Res. Rev. CSIRO Div. Mineral. 180–182.

Hall, G.E.M., Vaive, J.E., Beer, R., Hoashi, M., 1996. Phase selective leaches for use in exploration geochemistry. Bull. Geol. Surv. Can. 169–200, [Report 426].

Hoffman, P., 1988. United plates of America, the birth of a craton: Earl Proterozoic assembly and growth of Laurentia. Annu. Rev. Earth Planet. Sci. 16, 543–603.

Holk, G.J., Kyser, T.K., Chipley, D., Hiatt, E.E., Marlatt, J., 2003. Mobile Pb isotopes in Proterozoic sedimentary basins as guides for exploration of uranium deposits. J. Geochem. Explor 80, 297–320.

Kelley, D.L., Cameron, E.M., Southam, G., 2004. Secondary geochemical dispersion through transported overburden. Publ. Geol. Dep. Ext. Serv. Univ. West. Austr. 33, 93–96.

Kelley, D.L., Kelley, K.D., Coker, W.B., Caughlin, B., Doherty, M.E., 2006. Beyond the obvious limits of ore deposits: the use of mineralogical, geochemical, and biological features for the remote detection of mineralization. Econ. Geol. 101, 729–752.

Kelley, K.D., Hudson, T., 2007. Natural versus anthropogenic dispersion of metals to the environment in the Wulik River area, western Brooks Range, northern Alaska. Geochem. Explor. Environ. Anal. 7, 87–96.

Kozuskanich, J.C., Kyser, T.K., MacFarlane, W.R., Hamilton, S.M., 2009. Dendrochemical variation over the Cross Lake VMS mineralization a tool for mineral exploration and decoupling anthropogenic input from background signals. Geochem. Explor. Environ. Anal. 9, 151–157.

Kylander, M.E., Weiss, D.J., Kober, B., 2009. Two high-resolution terrestrial records of atmospheric Pb deposition from New Brunswick, Canada, and Loch Laxford, Scotland. Sci. Total Environ. 407, 1644–1657.

Kyser, K., 2012. Isotopes as tracers of elements across the geosphere–biosphere interface. In: Vanhaecke, F., Degryse, D. (Eds.), Isotopic Analysis: Fundamentals and Applications Using ICP-MS. Wiley-VCH Verlag GmbH & Co. KGaA, Weinheim, Germany, pp. 351–372.

Lageard, J.G.A., Howell, J.A., Rothwell, J.J., Drew, I.B., 2008. The utility of *Pinus sylvestris* L. in dendrochemical investigations; pollution impact of lead mining and smelting in Darley Dale, Derbyshire, UK. Environ. Pollut. (1987) 153, 284–294.

Lahd Geagea, M., Stille, P., Gauthier-Lafaye, F., Millet, M., 2008. Tracing of Industrial Aerosol Sources in an Urban Environment Using Pb, Sr, and Nd Isotopes. Environ. Sci. Technol. 42, 692–698.

Leslie, K., Oates, C.J., Kyser, T.K., Fowle, D.A., 2014. Biogeochemical controls on metal mobility: Modeling a Cu-Zn VMS deposit in column flow-through studies. Geochem. Explor. Environ. Anal. 14, 59–70.

Leybourne, M.I., Cousens, B.L., Goodfellow, W.D., 2009. Lead isotopes in ground and surface waters; fingerprinting heavy metal sources in mineral exploration. Geochem. -Explor. Environ. Anal. 9, 115–123.

Marlatt, J.L., Kyser, T.K., 2011. Paradigmatic shifts in the uranium exploration process; knowledge brokers and the Athabasca Basin learning curve. SEG Newsl. 84 (1), 17–23.

Patrick, G.J., Farmer, J.G., 2006. A stable lead isotopic investigation of the use of sycamore tree rings as a historical biomonitor of environmental lead contamination. Sci. Total Environ. 362, 278–291.

Percival, J.B., Bell, K., Torrance, J.K., 1993. Clay mineralogy and isotope geochemistry of the alteration halo at the Cigar Lake uranium deposit. Can. J. Earth Sci. 30, 689–704.

Plant, J.A., Ridgway, J., Hale, M., 1988. Developments in regional geochemistry for mineral exploration. Trans. I. Min. Metall. B 97, B116–B140.

Prohaska, T., Stadlbauer, C., Wimmer, R., Stingeder, G., Latkoczy, C., Hoffmann, E., Stephanowitz, H., 1998. Investigation of element variability in tree rings of young Norway spruce by laser-ablation-ICP-MS. Sci. Total Environ. 219, 29–39.

Ramaekers, P., Jefferson, C.W., Yeo, G.M., Collier, B., Long, D.G.F., Drever, G., McHardy, S., Jiricka, D., Cutts, C., Wheatley, K., Catuneanu, O., Bernier, S., Kupsch, B.G., Post, R., 2007. Revised geological map and stratigraphy of the Athabasca Group, Saskatchewan and Alberta. Bull. Geol. Surv. Can. 4, 155–191.

Reimann, C., Flem, B., Arnoldussen, A., Englmaier, P., Finne, T.E., Koller, F., Nordgulen, O., 2008. The biosphere: a homogeniser of Pb isotope signals. Appl. Geochem. 23, 705–722.

Shortle, W.C., Smith, K.T., Minocha, R., Lawrence, G.B., David, M.B., 1997. Acidic deposition, cation mobilization, and biochemical indicators of stress in healthy red spruce. J. Environ. Qual. 26, 871–876.

Shotyk, W., Krachler, M., 2010. The isotopic evolution of atmospheric Pb in central Ontario since AD 1800, and its impacts on the soils, waters, and sediments of a forested watershed, Kawagama Lake. Geochim. Cosmochim. Acta 74, 1963–1981.

Shotyk, W., Le Roux, G., 2005. Biogeochemistry and cycling of lead. Met. Ions Biol. Syst. 43, 239–275.

Shotyk, W., Weiss, D., Appleby, P.G., Cheburkin, A.K., Frei, R., Gloor, M., Kramers, J.D., Reese, S., Van der Knaap, W.O., 1998. History of atmospheric lead deposition since 12,370 C-14 yr BP from a peat bog, Jura Mountains, Switzerland. Science 281, 1635–1640.

Simonetti, A., Gariepy, C., Carignan, J., Poissant, L., 2000a. Isotopic evidence of trace metal sources and transport in eastern Canada as recorded from wet deposition. J. Geophys. Res. 105, 12263–12278.

Simonetti, A., Gariepy, C., Carignan, J., 2000b. Pb and Sr isotopic compositions of snowpack from Quebec, Canada: Inferences on the sources and deposition budgets of atmospheric heavy metals. Geochim. Cosmochim. Acta 64, 5–20.

Tessier, A., Gallon, C., Gobeil, C., Beaudin, L., 2005. Sources and chronology of atmospheric lead deposition to a Canadian Shield lake: inferences from Pb isotopes and PAH profiles. Geochim. Cosmochim. Acta 69, 3199–3210.

Velde, B., 1992. Introduction to Clay Minerals: Chemistry, Origins, Uses and Environmental Significance, first ed. Chapman & Hall, London; New York.

Warren, H.V., Delavault, R.E., Irish, R.I., 1952. Biogeochemical investigations in the Pacific Northwest. Geol. Soc. Am. Bull. 63, 435–484.

Watmough, S.A., 1997. Evaluation of the use of dendrochemical analyses in environmental monitoring. Environ. Rev. 5, 181–201.

Watmough, S.A., 1999. Monitoring historical changes in soil and atmospheric trace metal levels by dendrochemical analysis. Environ. Pollut. (1987) 106, 391–403.

Watmough, S.A., Hutchinson, T.C., 2003. A comparison of temporal patterns in trace metal concentration in tree rings of four common European tree species adjacent to a Cu-Cd refinery. Water Air Soil Pollut. 146, 225–241.

Weiss, D., Shotyk, W., Appleby, P.G., Kramers, I.D., Cheburkin, A.K., 1999. Atmospheric Ph deposition since the industrial revolution recorded by five Swiss peat profiles: enrichment factors, fluxes, isotopic composition, and sources. Environ. Sci. Technol. 33, 1340–1352.